Discover Applied Sciences

Research

Mapping dominant tree species of miombo woodlands in Western Tanzania using PlanetScope imagery

Siwa E. Nkya[1,2] · Deo D. Shirima[3,4] · Robert N. Masolele[5] · Henrik Hedenas[6] · August B. Temu[7]

Received: 1 July 2024 / Accepted: 3 October 2024
Published online: 06 October 2024

Abstract

Mapping dominant tree species in miombo woodlands is essential for enhancing their monitoring and management. We evaluated PlanetScope imagery to map *Julbernardia globiflora*, *Brachystegia spiciformis*, and *Pterocarpus tinctorius* in Tongwe Forest Reserve, Tanzania. The study assessed the effectiveness of PlanetScope bands in discriminating tree species and investigated how different months/seasons influenced tree species classification. Optimal months (seasons) and spectral bands were selected using Principal Component loading, temporal pattern analysis, mean decrease in accuracy, and mean decrease Gini techniques. Random forest classification was employed for tree species classification, and accuracy was assessed using an error matrix. The study identified March, July, and September as optimal months for acquiring imagery, with effective bands including blue, green-1, green, yellow, red, and red-edge. July and September imagery in the dry season achieved higher overall accuracies of 65% and 69%, respectively, while March imagery in the wet season reached 55%. The highest overall accuracy of 72% was achieved using images from different seasons. Producer's accuracy was highest for *Brachystegia spiciformis* (79%) and *Julbernardia globiflora* (95%), whereas *Pterocarpus tinctorius* had lower accuracy (25%). User's accuracy varied with 74% for *Brachystegia spiciformis*, 70% for *Julbernardia globiflora*, and 67% for *Pterocarpus tinctorius*. Mapping accuracy was notably high for *Brachystegia spiciformis* and *Julbernardia globiflora*, reflecting their high sample size (dominance) and distinct phenology. The yellow and red bands were particularly effective in distinguishing miombo tree species demonstrating PlanetScope's capability. Future research should focus on scaling up PlanetScope's application for broad miombo tree species mapping.

Article Highlights

- Multi-season imagery enhances the accuracy of mapping dominant miombo tree species.
- Yellow and red spectral bands are the most effective in discriminating miombo tree species.
- PlanetScope reliably maps populations of the dominant species *Brachystegia spiciformis* and *Julbernardia globiflora*.

Supplementary Information The online version contains supplementary material available at https://doi.org/10.1007/s42452-024-06248-8.

✉ Siwa E. Nkya, nkyasiwa@gmail.com | [1]Regional Research School in Forest Sciences (REFOREST), College of Forestry, Wildlife, and Tourism, Sokoine University of Agriculture, P.O. Box 3009, Chuo Kikuu, Morogoro, Tanzania. [2]Tanzania Forestry Research Institute, P.O Box 1854, Morogoro, Tanzania. [3]Department of Ecosystems and Conservation, College of Forestry, Wildlife, and Tourism, Sokoine University of Agriculture, P.O. Box 3010, Chuo Kikuu, Morogoro, Tanzania. [4]National Carbon Monitoring Centre, Sokoine University of Agriculture, P.O. Box 3009, Chuo Kikuu, Morogoro, Tanzania. [5]Laboratory of Geo-Information Science and Remote Sensing, Environmental Sciences Group, Wageningen University and Research, Postbus 47, 6700AA Wageningen, The Netherlands. [6]Department of Forest Resource Management, Swedish University of Agricultural Sciences, S.E.—901 83 Umeå, Sweden. [7]College of Forestry, Wildlife, and Tourism, Sokoine University of Agriculture, P.O. Box 3009, Chuo Kikuu, Morogoro, Tanzania.

Keywords Unmanned aerial vehicle (UAV) · Temporal pattern analysis · Principal component analysis (PCA) · Mixed forests · Variable importance · Random forest

1 Introduction

Miombo refers to woodlands dominated by tree genera Brachystegia, Julbernardia, and/or Isoberlinia from the legume family Fabaceae, subfamily Caesalpinioideae [1]. These woodlands are extensive tropical dry forests covering 2 million square kilometers across Angola, Malawi, Mozambique, Tanzania, Zimbabwe, Zambia, and the Democratic Republic of Congo [2]. The miombo ecosystems harbor 8,500 plant species, of which over 54% are endemic [1]. This plant diversity is crucial for providing household energy, timber, and food such as mushrooms, fruits, and honey, sustaining income through beekeeping, and supporting crop pollination [3–5].

The rising demand for woodland products and the expansion of cropland due to population growth are leading to woodland loss [6, 7] and loss of miombo tree species [8].These drivers could potentially affect the dominant species, which determine the properties of the miombo ecosystem [8, 9]. Dominant tree species are large, coarse-grained resource foragers that significantly contribute to plant biomass in specific vegetation types [10]. According to mass ratio theory, these species play a major role in ecosystem functions and sustainability [10]. Therefore, the decline and loss of dominant tree species signify a decline in ecosystem functions and the benefits they provide to humans.

Given the unprecedented rate of woodland loss and the potential threat of climate change [11, 12], it is imperative to effectively manage miombo-dominant tree species to uphold the health and stability of the miombo ecosystem. However, the current reliance on labor-intensive and costly ground surveys in Tanzania for essential data hinders consistent and comprehensive monitoring. Remote sensing technologies offer a practical and cost-effective alternative, enabling frequent and extensive monitoring of large areas to accurately assess the distribution of dominant tree species [13].

To map dominant tree species in miombo woodlands, sensors with very high spatial, spectral, and temporal resolutions are essential. These sensors capture details of canopy structure, internal leaf structure and biochemicals, and phenological variations between tree species [14]. Consequently, multi-date and multispectral Unmanned Aerial Vehicle (UAV) imagery—including blue, green, red, red-edge, and near-infrared bands—was used to track dominant tree species in the wet miombo woodlands of Zambia [15]. It is important to note that while UAV imagery provides very high spatial resolution, it is limited to mapping small areas, such as plots or fields [16].

Mapping tree species on a large scale requires Very High-Resolution (VHR) satellite data [14]. WorldView-2 imagery was used to map seven common savanna tree species with large crowns in South Africa, achieving an overall accuracy of 77% ± 3.1 [17]. Quickbird imagery was used to discriminate five indigenous tree species in woodlands within Palapye, Botswana, with an overall accuracy of 88.7% [18]. Additionally, WorldView-2 imagery was used to discriminate four tree species in the savannah vegetation of South Africa, achieving the highest overall accuracy of 80% [19].Moreover, using multi-seasonal imagery significantly improved the classification accuracy of tree species [15]. Multi-seasonal imagery enhanced accuracy, particularly when acquired during the transition from wet to dry season in the savannah vegetation of South Africa [19]. Additionally, multi-seasonal images improved the mapping of nine wetland and dryland communities in KwaZulu-Natal, South Africa, achieving a high overall accuracy of 86 ± 2.8% using RapidEye imagery (5-m spatial resolution) [20].

To comprehensively leverage the phenological data of tree species, it is imperative to utilize high-resolution satellite sensors such as PlanetScope. With its daily global revisit capability and a range of spectral bands including coastal blue, blue, green, green I, yellow, red, red edge, and near-infrared, PlanetScope imagery is strategically positioned for effective tree species and vegetation monitoring. Recent studies have demonstrated the utility of PlanetScope imagery in mapping tree species based on their phenological variations [21]. Nevertheless, there remains a paucity of efforts to harness the potential of PlanetScope for mapping dominant tree species within miombo woodlands.

This study assessed PlanetScope's utility for mapping dominant tree species in the wet miombo of Western Tanzania by exploiting their seasonal phenological differences. The following research questions guide the study in meeting its objective: (i) What is the optimal month and season for acquiring images to discriminate tree species? (ii) Which PlanetScope bands help discriminate miombo dominant tree species? (iii) Does the use of multi-date, including multi-season, improve miombo dominant tree species classification?

2 Material and methods

2.1 Study area

The study was conducted on a 9-hectare site within the Tongwe West Forest Reserve (TWFR) in the Tanganyika District of the Katavi Region (Fig. 1). The site is located at longitude 30° 29′ 13″ E and latitude 5° 27′ 41″ S, with an elevation of 1490 m above sea level. TWFR experiences minimum and maximum annual temperatures of 15 °C and 25 °C, respectively, with a yearly total rainfall of 1210 mm [22]. The rainfall pattern at the site is unimodal, beginning in November and ending in May of the following year. Due to the total annual rainfall exceeding 1,000 mm, the site is predominantly categorized as awet miombo.

2.2 Study species

We selected three miombo tree species to map within the 9-hectare study area. *Brachystegia spiciformis* (Mtundu) and *Julbernardia globiflora* (Muva) were chosen as the two most dominant species in this area. *Pterocarpus tinctorius* (Mkurungu), a valuable timber species listed under CITES Appendix II, was selected due to its contribution to the biomass of the 9-hectare area, ranking just after *Brachystegia spiciformis* and *Julbernardia globiflora*.

Brachystegia spiciformis and *Julbernardia globiflora* are not only dominant locally within the 9-hectare study area, but they are also two of the most common species regionally in the miombo woodland of Western Tanzania. This is supported by a survey carried out in the Tabora and Sikonge districts of the Tabora Region, as well as in the Mlele and Tanganyika districts of the Katavi Region, in 2022 and 2023. The current survey employed a two-stage sampling design, with 52 grids chosen in the first stage based on Woodland Cover, NDVI, Elevation, Rainfall, Soil Moisture Index, Soil Organic Carbon, Total Nitrogen, and Total Phosphorous variables using a spatially balanced design. Within each grid, up to three plots measuring 30 × 30 m

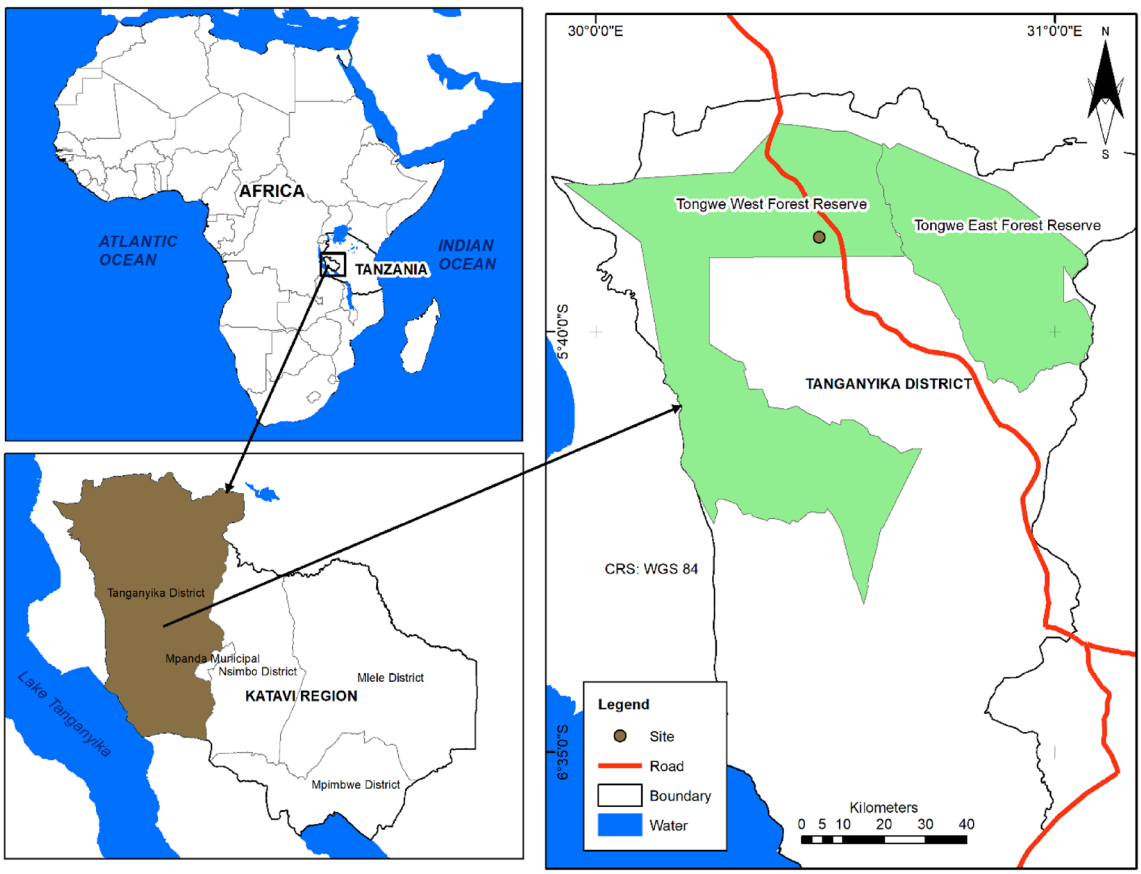

Fig. 1 Location of the site within the Tongwe Forest Reserve in the Tanganyika District, Katavi Region, Tanzania

were randomly selected in the second stage, resulting in a sample size of 152 plots, sufficient to estimate the floristic composition (Fig. 2).

In these plots, trees with a diameter ≥ 5 cm were identified and measured for Diameter at Breast Height (DBH). The observed number of species was 148, and according to Chao1, Jackknife, and Bootstrap measures, the estimated number of species ranged between 159 and 185.

In this study, the Importance Value Index (IVI) was used to assess species dominance within a community. The IVI measures the relative importance of species based on their frequency, density, and dominance (basal area). It is calculated by summing the relative frequency (RF), relative density (RD), and relative dominance (RD) of each species.

The formula used to calculate relative values for each species were:

$$\textit{Relative Frequency}\,(RF) = \frac{\textit{Number of plots in which a species occurs}}{\textit{Number of plots in which a species occurs summed for all species}} \times 100$$

$$\textit{Relative Density}\,(RD) = \frac{\textit{Number of individuals of each species per plot area}}{\textit{Number of individuals of each species per plot area summed for all species}} \times 100$$

$$\textit{Relative Dominance}\,(RD) = \frac{\textit{Basal area of each species per plot area}}{\textit{Basal area of each species per plot area summed for all species}} \times 100$$

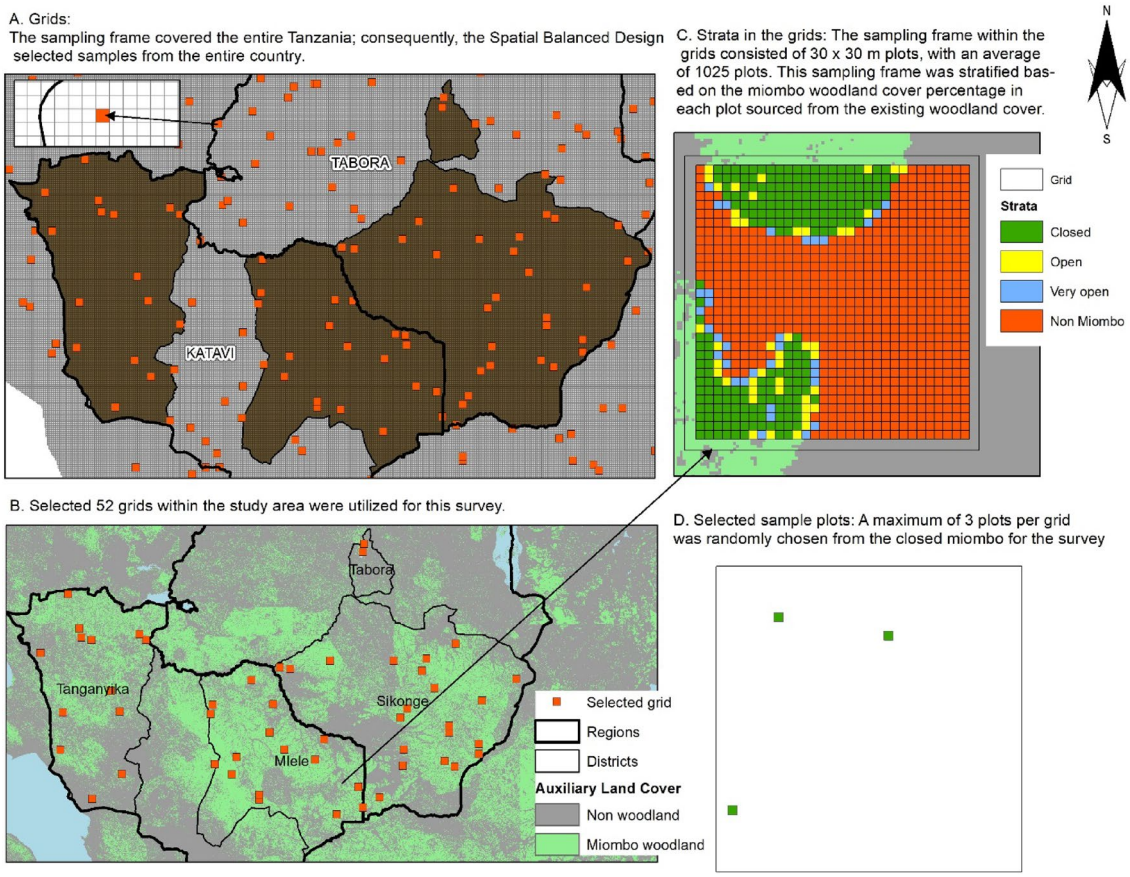

Fig. 2 An illustration of the stages involved in the sampling design: **A** The sampling frame (grid 1 × 1 km^2) and 1000 grids were randomly selected from this frame using a balanced sample in the first stage, covering the entire Tanzania. **B** Selected 52 grids within the study area. **C** Plots within the grids were automatically classified based on auxiliary canopy cover and used as sampling classes. **D** Sample plots were randomly selected from the closed miombo–Miombo woodlands with the canopy cover above 70%

However, in this study, the importance value index (IVI) was calculated using the importancevalue function of BiodiversityR package in R software.

Results from the importance value index (IVI) of tree species indicated that *Brachystegia spiciformis*, *Julbernardia globiflora*, and *Pterocarpus tinctorius* ranked first, second, and seventeenth, respectively (Appendix 1).

The target species are deciduous trees belonging to the Fabaceae family. The observed distinctive features of these trees in the study area were as follows:

- *Julbernardia globiflora* has light red young leaves from August to September and yellow-white flowers in February and March.
- *Brachystegia spiciformis* produces red/pink young leaves from August to September before the rains. Its green flowers, easily mistaken for leaves, emerge during the leaf flush period of August to September.
- *Pterocarpus tinctorius* produces golden yellow flowers from March to May.

2.3 Methods

Figure 3 provides a flowchart of the applied methods.

2.3.1 Step 1: sampling of tree crowns for training and validation

Training data collection is a prerequisite in supervised image classification. These data guide the classifier in determining specific spectral values for the training, which the classifier will use to map the distribution of the classes/species. In this study, canopy trees of interest were identified in the field, and their locations were captured using differential GPS. Additionally, drone images were acquired to identify and digitize the crowns of the identified trees and to digitize woodland and non-woodland areas. Seventy per cent of the digitized crowns per tree species were used to train the classifier, while 30% were used to validate the classifier in mapping dominant miombo tree species. The process involved the following steps:

2.3.1.1 Identifying and capturing tree location The site was divided into nine 1-hectare plots. Within each plot, canopies of dominant tree species were selected based on the following features: solitary tree crowns, tree crowns with no interlocking with other tree species' crowns, the concentration of tree crowns of the same species in an area, and the presence of flowers in tree crowns (e.g., *Julbernardia globiflora* and *Pterocarpus tinctorius* crowns). The concentration of tree crowns of the same species was crucial in enhancing the species' canopy cover, as Cho et al. (2010) found that the crown of the tree species to be mapped should be at least three times the size of the image's pixel to be used for mapping. Other tree species besides the target species were grouped separately. Selected tree species were measured for diameter at breast height (DBH), and their locations in the plots were captured by Differential GPS (DGPS).

2.3.1.2 Acquiring drone imagery The DJI-MAVIC Air 2 camera captured imagery on 13 March 2024. Drone images were gathered between 08:30 am and 09:15 am (East African Time, Nairobi) in an east–west pattern at a ground speed of 15.7 km/hr and a height of 40 m. We collected 1032 frames with 80% forward and 80% side overlaps, and a quality score above 0.5 (ranging from 0 to 1), to build accurate and detailed orthophotos at a spatial resolution of 1 cm. Moreover, we deployed 16 Ground Control Points (GCPs) georeferenced with a differential GPS (DGPS) to enhance the alignment of the cameras and geometric accuracy.

Drone imagery was processed using Agisoft Metashape Professional software. High alignment was applied to align the cameras with placed markers and Ground Control Points to enhance geometric accuracy. Additionally, high-quality settings were used to build dense clouds. Following this, a digital elevation model and orthomosaic were created. The crowns of sampled trees were digitized from the orthomosaic, guided by the tree location data collected during sampling (Fig. 4). Tables 1 show the tree species' sampled crown areas (m^2).

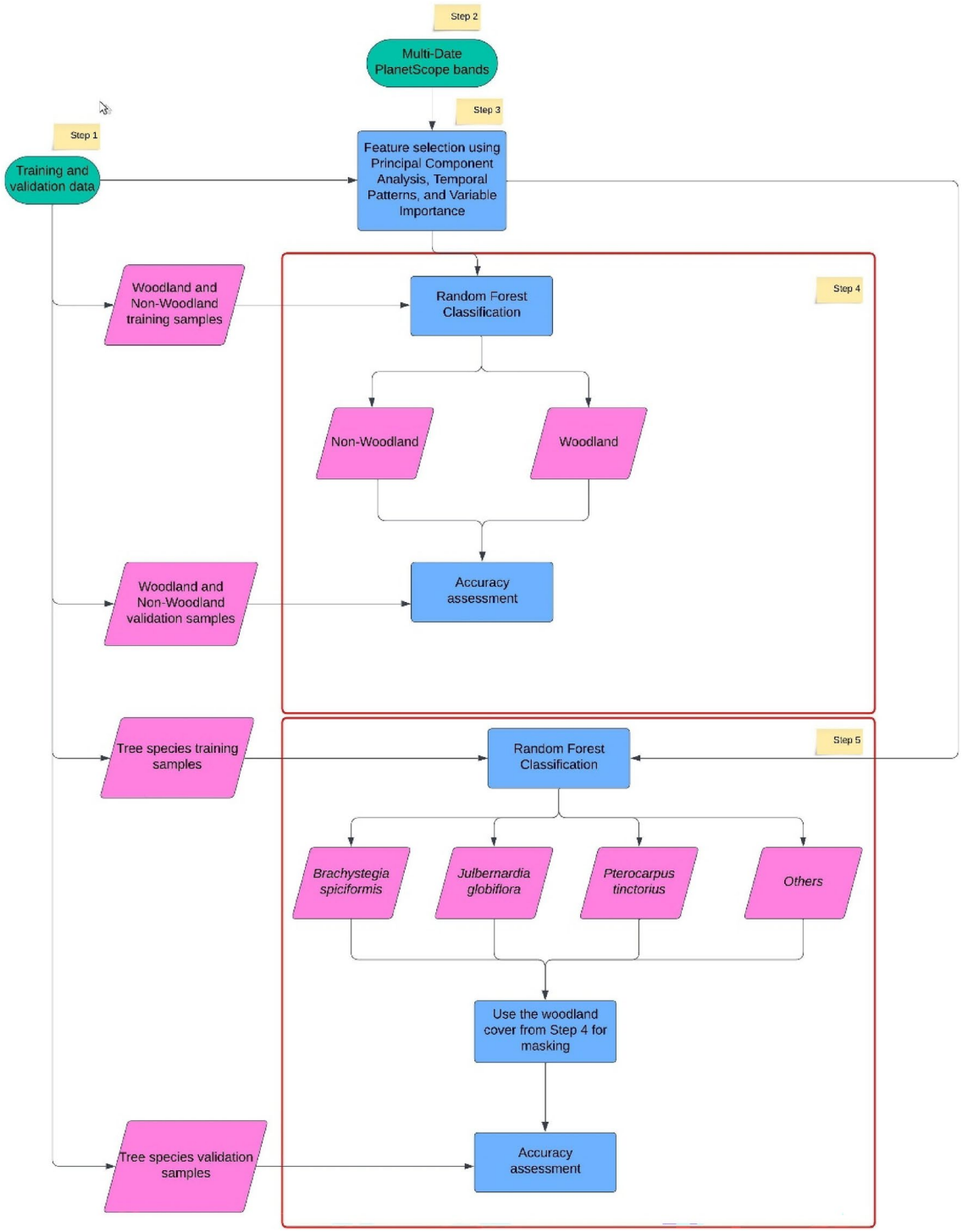

Fig.3 A flowchart of the applied methods. Step 1 involved collecting reference data. Step 2 involved acquiring PlanetScope spectral bands. Step 3 involved feature selection to map miombo-dominant tree species. Step 4 involved mapping woodland cover. Step 5 involved mapping tree species

2.3.2 Step 2: model training feature

We acquired cloud-free PlanetScope images for the year 2023 from Planet Labs obtained through a research license. PlanetScope operates in coastal blue, blue, green, green I, yellow, red, red edge, and near-infrared bands. These bands were used as features in mapping woodland and non-woodland areas, as well as the dominant miombo tree species.

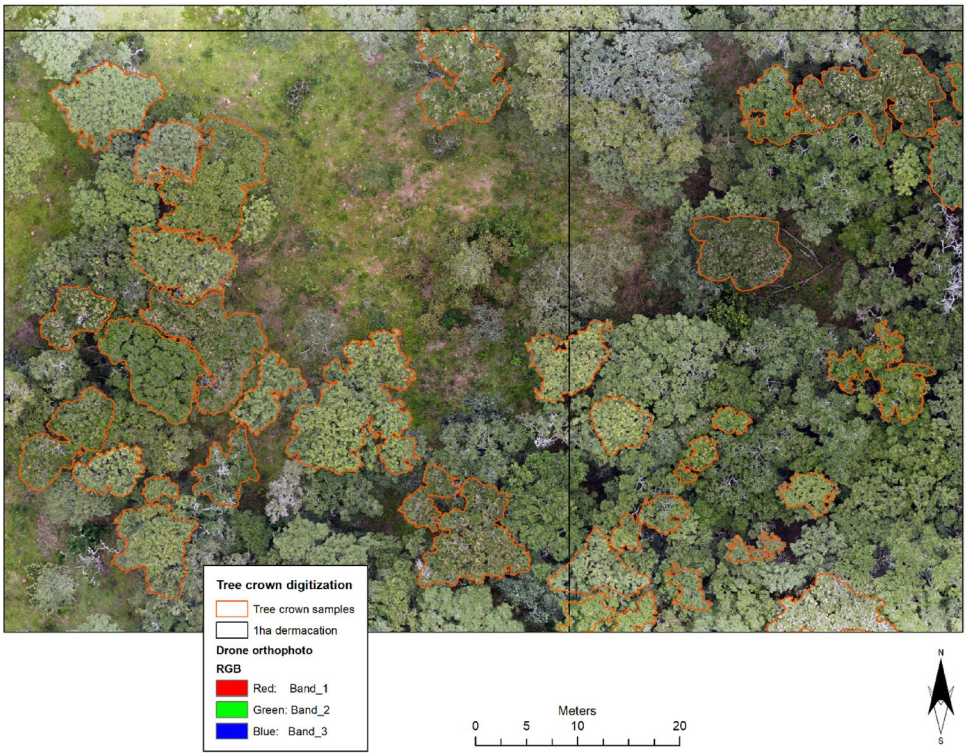

Fig. 4 Illustrations of tree crown digitization from the drone orthomosaic

Table 1 Samples collected per dominant tree species in the study area

Species	Sampled crown					
	Total				Minimum area of 9 m^2	
	Number of sampled crown	Crown area (m^2)	Crown area (m^2) used for training	Crown area (m^2) used for validation	Number of sampled crown	Crown area (m^2)
Julbernardia globiflora	128	4941	3966	975	116	4876
Brachystegia spiciformis	111	5370	4279	1091	95	5281
Pterocarpus tinctorius	50	2277	1708	569	45	2263
Other species (Control)	13	492	290	202	13	492

We used the digitized layers to extract bi-monthly reflectance values from the PlanetScope spectral bands for both woodland and non-woodland covers, as well as tree species.

2.3.3 Step 3: feature selection

We selected optimal features for distinguishing miombo/non-miombo areas and dominant miombo tree species.

2.3.3.1 Determination of optimal months and optimal spectral bands The optimal months and spectral bands for mapping tree species were determined by analyzing all the bands from bi-monthly PlanetScope imagery for the year 2023 using Principal Component Analysis (PCA), Temporal Pattern Analysis, Mean Decrease in Accuracy (MDA), and Mean Decrease in Gini (MDG) in R software. PCA with the prcomp function identified the layer that best separated the tree species. Principal Component (PC) loading was used to extract bands that contributed most to this separation. The temporal pattern analysis displayed trends of spectral band values of the tree species over the dates of 2023, highlighting the bands and months that differentiated the species. MDA and MDG, as random forest metrics, determined important variables [23, 24]. The MDA and MDG validated observations from PCA and Temporal Pattern Analysis.

2.3.4 Step 4: woodland and non-woodland classification

The random forest classifier in R software was used to map woodland and non-woodland covers from the optimal PlanetScope imagery. Temporal pattern analysis (Fig. 5), PCA (Fig. 7a), MDA (Fig. 9a), and MDG (Fig. 9a) collectively identified March, May, June, and October as the optimal months for acquiring satellite imagery to distinguish between woodland and non-woodland areas. The most significant bands were yellow, red and Red edge (FigS. 7b and 9a, displaying the top 10 and 15 most important bands out of 168, respectively). Based on these results, an image from early June, at the start of the dry season, was selected to create a woodland mask.

The classifier was trained using 70% of the woodland training data and validated with the remaining 30%. The map in Fig. 6b was produced with an overall accuracy of 88.5%. The producer accuracies for woodlands and non-woodlands were 90.6% and 76.47%, respectively, with user accuracies of 95.6% and 59.09%.

2.3.5 Step 5: tree species classification

The random forest classifier in R was used to map dominant tree species from mono-temporal and multi-temporal PlanetScope images. The mono-temporal images were the color composite images from optimal months, while the multi-temporal images were stacks of bands from the color composite images of these months. The random forest classifier was trained using 70% of the crown data for each tree species group—*Brachystegia spiciformis*, *Julbernardia globiflora*, *Pterocarpus tinctorius,* and others. The remaining 30% of the crown data was used to validate the tree species maps (Table 1).The random forest classifier is a popular non-parametric machine-learning method that aims to find the best tree structure. It is known for its high classification accuracy, ease of determining important features, and ability to capture complex interactions among features, which is particularly useful when the spectral variation between classes is low. Additionally, it is less sensitive to overfitting [14, 25].

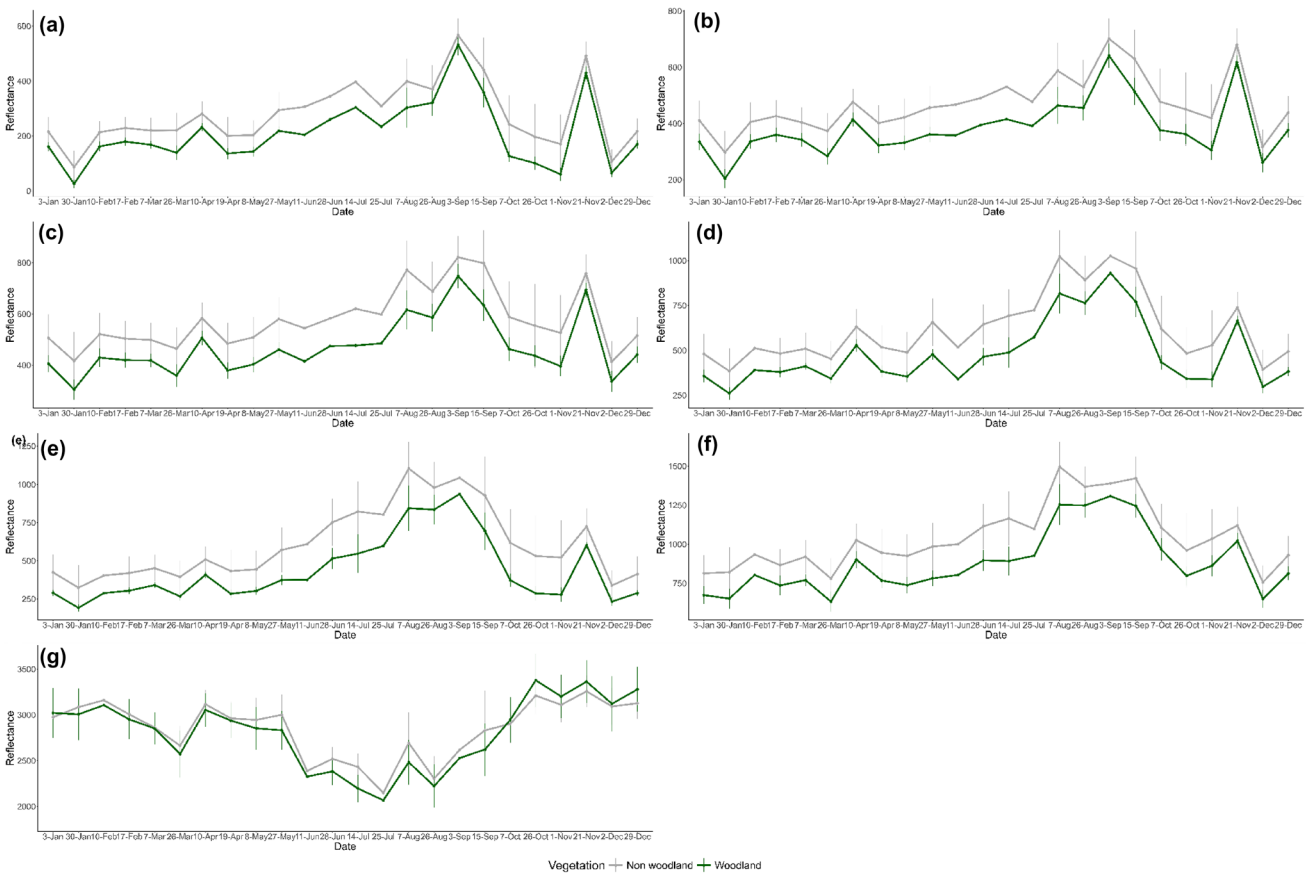

Fig. 5 Temporal curves of (**a**) Blue, (**b**) Green 1, (**c**) Green, (**d**) Yellow, (**e**) Red, (**f**) Red Edge, and (**g**) Near Infrared for Non-Woodland and Woodland based on PlanetScope images from 2023

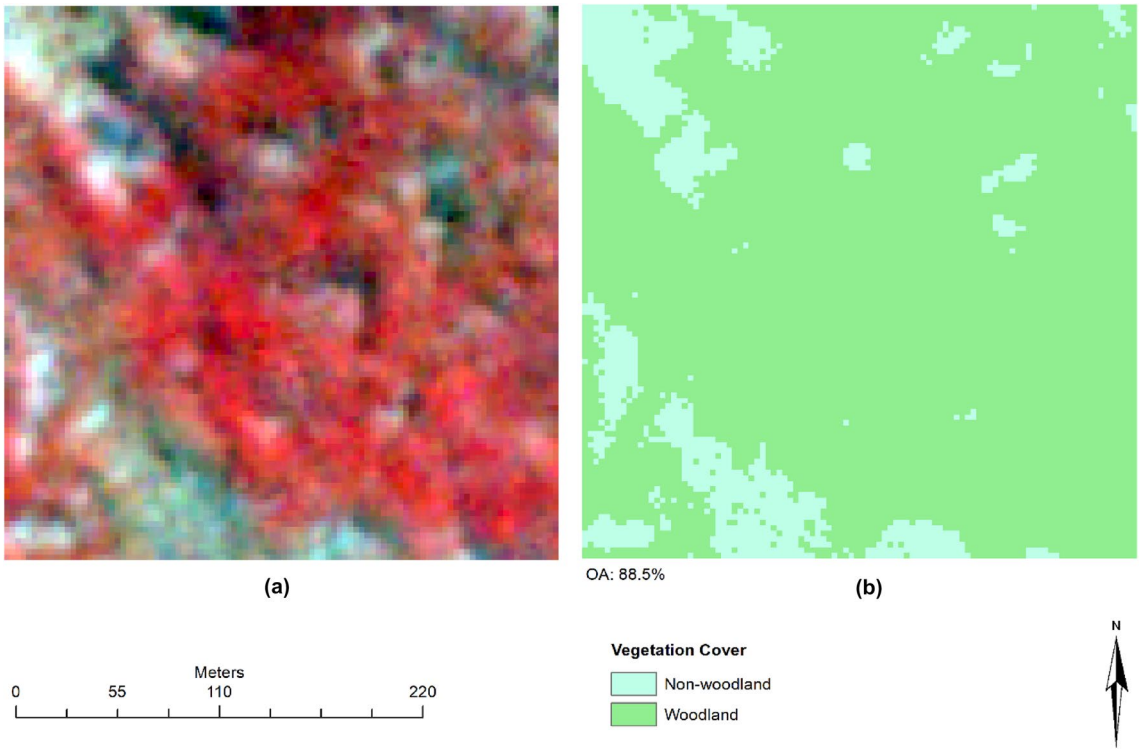

Fig. 6 **a** Raw color infrared PlanetScope image of the site. **b** Woodland/non-woodland classification map

The accuracies of the classifications were assessed using an error matrix, which provides information on the overall,producer's and user's accuracies. Based on this information, the classification with the highest accuracy was identified.

3 Results

3.1 Important months for mapping tree species

Tree species were better separated along dimension 2 (PC2) (Fig. 7c). The distinction between species was more pronounced between *Brachystegia spiciformis* and the rest. In contrast, *Julbernardia globiflora*, *Pterocarpus tinctorius*, and the control group (others) exhibited substantial overlap. The images that contributed significantly to dimension 2 (PC2) were from March in the wet season and July and September in the dry season (Fig. 7c, displaying the top 10 and 15 most important bands out of 168), respectively. The temporal pattern analysis results revealed that the separation between tree species was more pronounced during the dry season (defoliating period) from the end of June to mid-September (Fig. 8a–f). Based on the Mean Decrease in Accuracy (MDA) and Mean Decrease in Gini (MDG) results, the most important images for classifying tree species were from July and September in the dry season.

Due to these results, images from March in the wet season, and from July and September in the dry season, were selected as optimal for mapping tree species.

3.2 Important bands for mapping tree species

According to PCA, the most important bands that contributed to the separation of tree species in dimension 2 were the blue and red bands (Fig. 7d). Meanwhile, the blue, green-1, green, yellow, red, and red-edge bands contributed to the separation of tree species from the end of June to mid-September (dry season) according to the temporal pattern analysis. During this period, these bands, particularly the red band (Fig. 8e), exhibited the highest reflectance for *Brachystegia spiciformis* and the lowest for *Julbernardia globiflora*. Moreover, the near-infrared band was observed to discriminate the tree

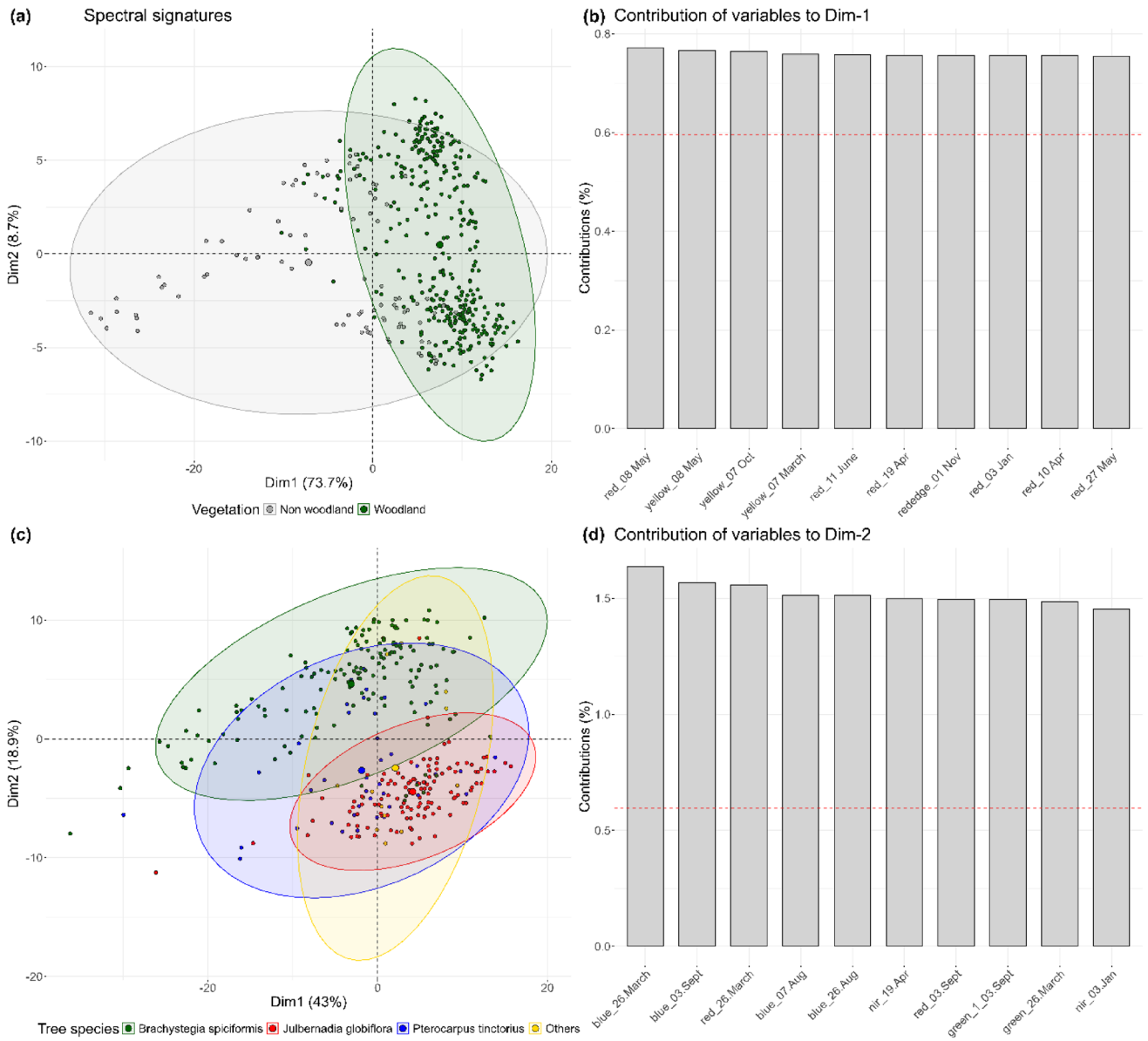

Fig. 7 **a** Principal Component Analysis (PCA) of Non-Woodland and Woodland, **b** Input PlanetScope layers that contribute significantly to the 73.7% variation explained by Principal Component 1 in distinguishing between non-woodland and woodland, **c** Principal Component Analysis (PCA) of Dominant tree species, **d** Input PlanetScope layers that contribute significantly to the 27.7% variation explained by Principal Component 2 in distinguishing between the dominant tree species in the year 2023

species with the highest reflectance for *Brachystegia spiciformis* and the lowest for *Julbernardia globiflora* from mid-April to early May at the end of the rainy season (Fig. 8). The important bands identified by MDA and MDG for distinguishing between tree species were yellow, red, and near infrared (NIR), with the yellow band being the most optimal (Fig. 9b).

Based on these results, the blue, green-1, green, yellow, red, and red-edge bands were selected as the optimal bands to discriminate between tree species.

3.3 Accuracy of utilizing images from optimal months compared to their multi-month combinations for tree species classification

Results revealed that images acquired in the dry season, especially in September, were the best for classifying tree species (Table 2). Utilizing images acquired in the wet season produced the lowest accuracy in mapping tree species. However, combining images from the wet season with those from the dry season yielded the highest accuracy in tree

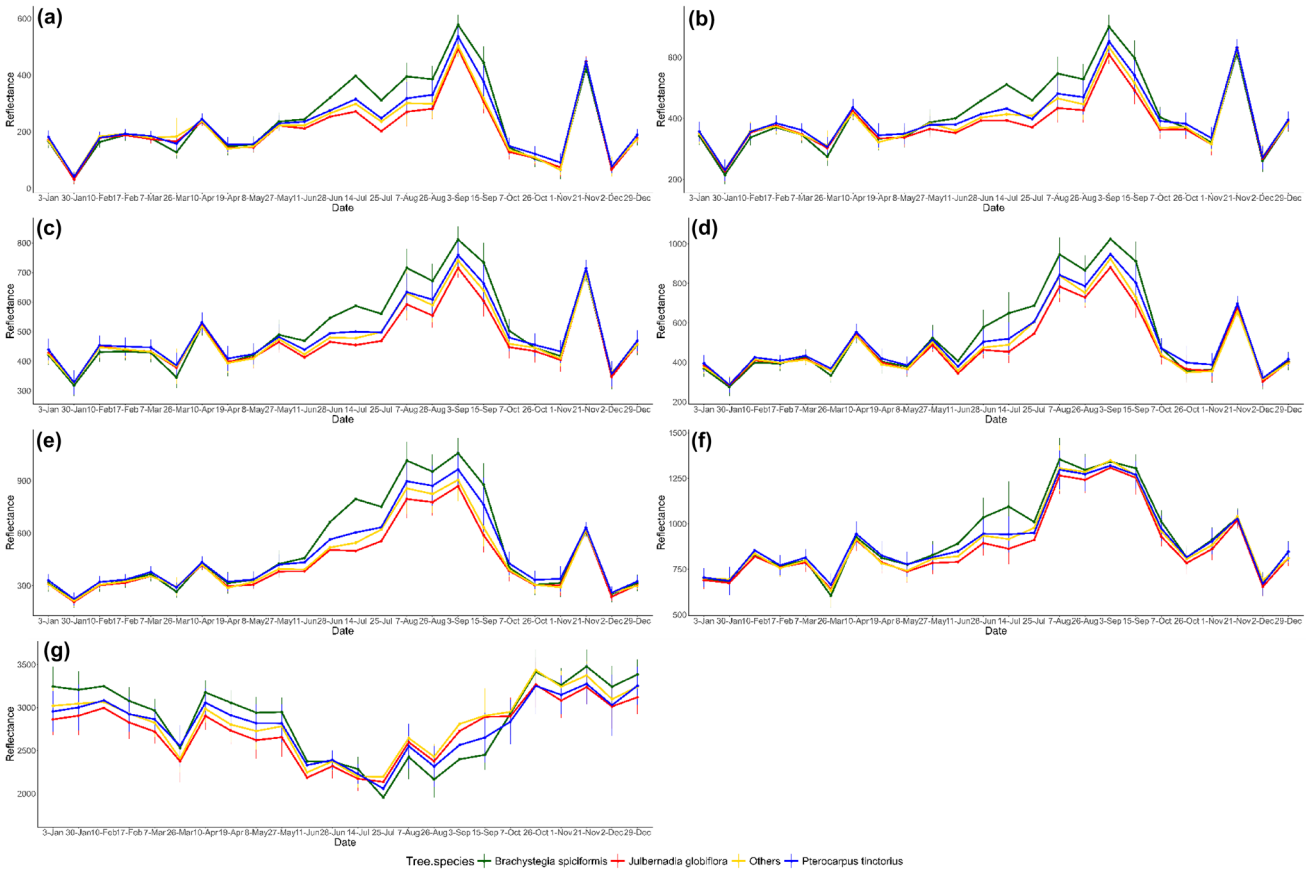

Fig. 8 Temporal curves of **a** Blue, **b** Green 1, **c** Green, **d** Yellow, **e** Red, **f** Red Edge, and **g** Near Infrared, for the dominant tree species based on PlanetScope images from 2023

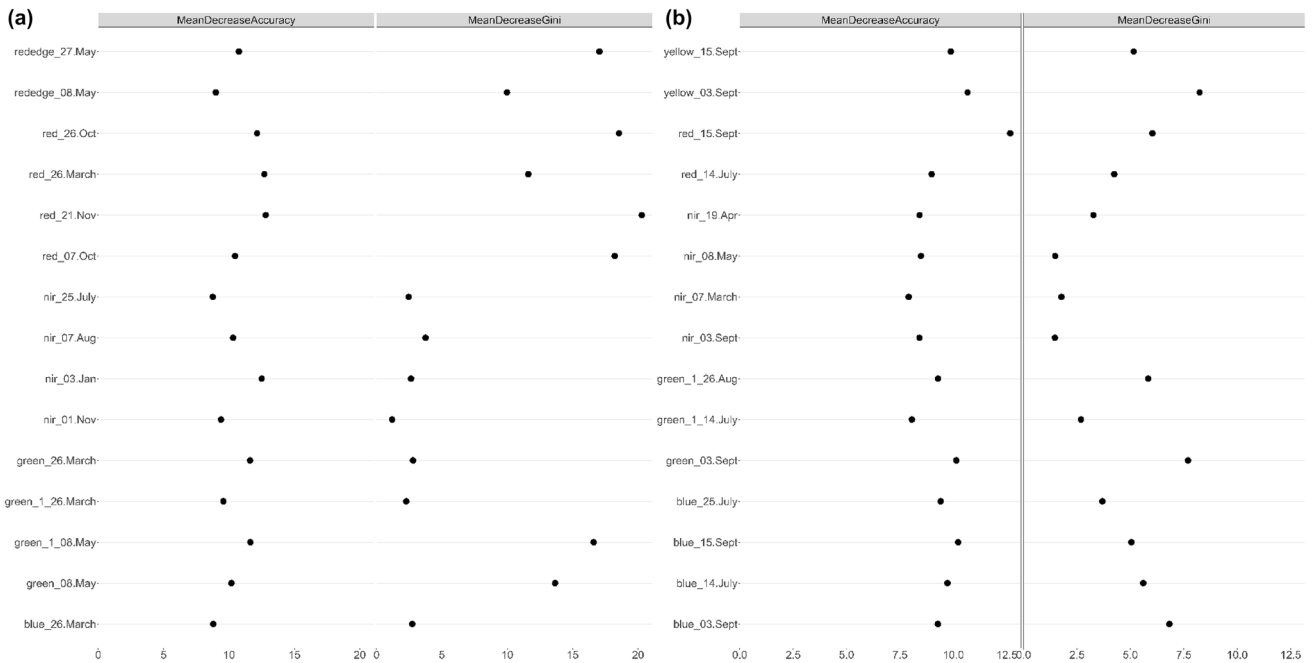

Fig. 9 The fifteen most important variables according to Mean Decrease Accuracy for **a** Woodland/Non-Woodland classification and **b** Miombo dominant tree species classification

Table 2 Overall accuracy in random forest for tree species classification using selected temporal images

Month (s)	Season (s)	Overall accuracy (%)
March	Wet	55
July	Dry	65
September	Dry	69
March/July	Wet/Dry	72
March/September	Wet/Dry	72
July/September	Dry/Dry	67
March/July/September	Wet/Dry/Dry	68

species mapping, particularly using combinations like March and July or March and September. Using multi-date images acquired within a single season, such as the dry season, resulted in lower accuracy compared to using multi-season images. Adding an image from another month within the dry season, such as July, to the multi-season combination did not improve tree species classification.

Furthermore, the Producer's and User's accuracies for mapping *Brachystegia spiciformis* and *Julbernardia globiflora* were high across all classifications (Fig. 10). However, these accuracies were higher in classifications utilizing images acquired in July and September (the dry season) compared to those utilizing images acquired in March (the wet season). Despite generally low Producer's and User's accuracies for mapping *Pterocarpus tinctorius*, images acquired in March (the wet season) had the highest accuracy for mapping this species.

The Producer's accuracy for mapping *Brachystegia spiciformis*, *Julbernardia globiflora*, and *Pterocarpus tinctorius* from the multi-season combination of March and September was 79%, 95%, and 25%, respectively. The User's accuracy was 74%, 70%, and 67%, respectively (Fig. 11) (Appendix 2).

4 Discussions

4.1 Optimal months to acquire PlanetScope imagery for tree species mapping

Images acquired during the dry season, particularly July and September, contributed highly to species classification due to leaf phenological changes. During this period, carotenoid levels increase in the miombo woodlands as leaves dry and fallen leaves on the ground become more exposed (cf. [26]).

August, during the dry season, was identified as the optimal month for acquiring images to distinguish dominant tree species in Zambia's wet miombo woodlands. Conversely, in the transition from the wet to dry season, April was found to be optimal for separating savanna tree species in South Africa [19]. However, both studies lacked images covering all months of the year. In the dry season within Western Tanzania's wet miombo, *Brachystegia spiciformis* exhibits the highest reflectance, followed by *Pterocarpus tinctorius* and *Julbernardia globiflora*. This pattern indicates physiological differences in coping with the dry season, with *Brachystegia spiciformis* shedding its leaves earlier than the other species.

4.2 Optimal bands from PlanetScope imagery to use for tree species mapping

The yellow band in the visible spectrum is the most significant for classifying tree species. Other vital bands include greens (green—1 and green), blue, and red within the visible spectrum, as well as the red-edge band outside the visible spectrum. Reflectance in these bands, particularly in yellow, increases during the dry season as carotenoid levels rise and chlorophyll—the pigment that absorbs them—declines. The yellow band significantly improved the classification accuracy of savanna tree species in South Africa [17, 19]. Similarly, the red band greatly enhanced the accuracy of mapping tree species in the South African savannah and Zambian wet miombo woodlands [15, 19]. The red edge band was also effective for mapping wet miombo-dominant tree species in Zambia [15]. These results highlight the importance of the yellow and green- 1 bands, which are absent in very high spatial resolution satellites with only four bands, for mapping dominant miombo tree species. Therefore, the blue, green—1, green, yellow, and red bands should be considered

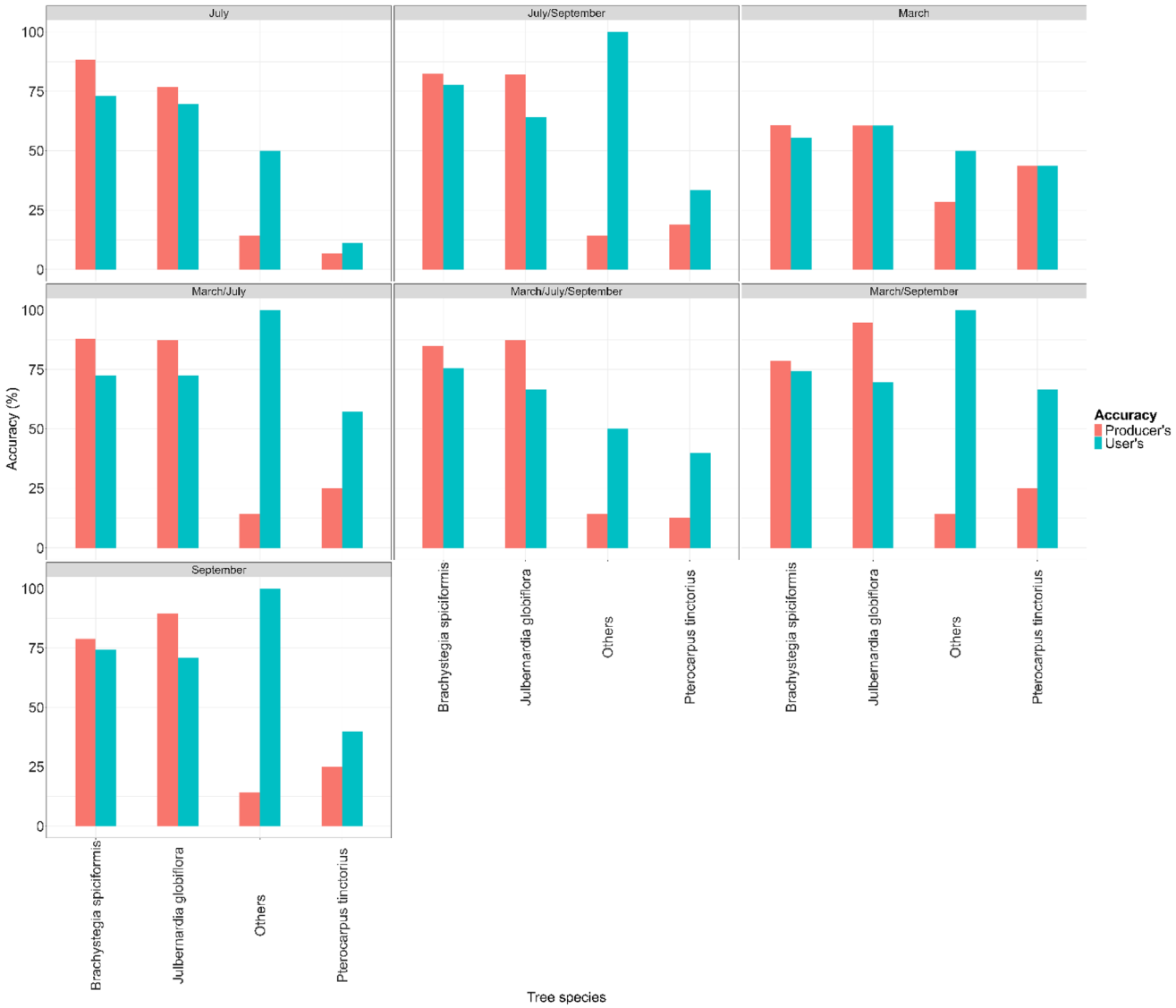

Fig. 10 Producer's and User's accuracies in mapping tree species using temporal images in the Year 2023

when mapping tree species in miombo woodlands, aligning with the emphasis on choosing optimal bands for high accuracy [27].

4.3 Accuracy of utilizing images from optimal months compared to their multi-month combinations for tree species classification

The results indicated that the highest overall accuracy of 72% was achievable from multi-season image combinations. For a single season, the highest classification accuracy of 69% was obtained from the image acquired in September. Using multi-seasonal images yields the highest accuracy as it captures phenological variations of tree species across seasons. Combining multi-date images from key phenological stages of dominant miombo tree species in Zambia resulted in higher classification accuracy than using images from a single optimal period [15]. Similarly, in other vegetation types, seasonal spectral features were found to outperform single-date features in classifying tree species [19–21, 28, 29]. Consequently, multi-season images should be considered for mapping miombo tree species.

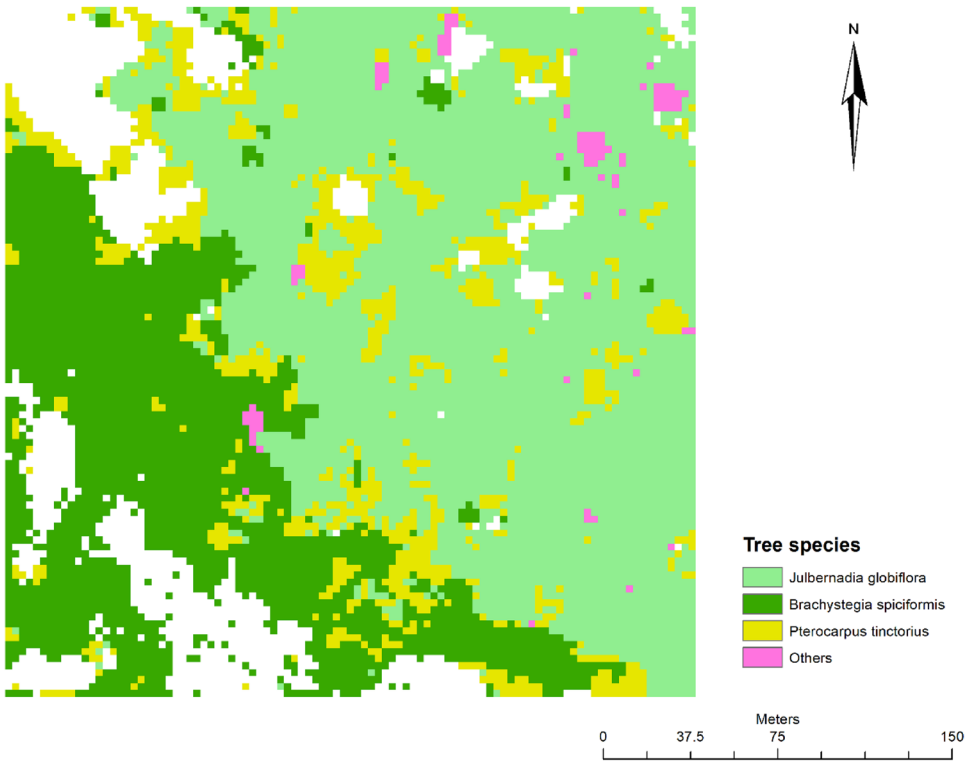

Fig. 11 The distribution of the dominant tree species obtained from the random forest classification of the combined images from March and September. The overall accuracy was 72%

In general, the accuracy of mapping tree species increases sequentially from others to *Pterocarpus tinctorius*, *Brachystegia spiciformis*, and *Julbernardia globiflora*, reflecting the high sample size (dominance) of *Julbernardia globiflora* and *Brachystegia spiciformis* and their distinct phenology at the site. Mapping accuracy was highest for *Julbernardia globiflora* which had the highest sample size, and lowest for other species with smaller sample sizes.

The results of this study provide effective processes and tools for mapping dominant tree species in miombo woodlands using PlanetScope, overcoming the current constraints of using moderate-resolution satellite data like Sentinel and Landsat. These processes could guide drone-based mapping of dominant tree species at the field scale. This will improve knowledge of tree species distribution, abundance, and traits over time. Enhancing species-oriented management is crucial for sustaining tree species amid deforestation and climate change challenges. Although the mean spectral values of tree species were distinct, individual spectral values were highly variable and nearly overlapping. This limitation was addressed by employing non-parametric random forest classification in tree species classification (cf. [27]).

5 Conclusions

Classifications using dry season images were more accurate than those using wet season images. The best mono-temporal imagery for tree species mapping was acquired in September, during the dry season. The optimal PlanetScope bands for classifying dominant tree species were blue, green-1, green, yellow, red, and red-edge. Additionally, classifications using multi-season images from March and July, as well as from March and September, yielded the highest accuracy in tree species classification. Mapping accuracy increased with the dominance of the tree species at the site. Based on these results, we recommend further research to apply this methodology for mapping dominant tree speciespopulations across extensive miombo woodland areas.

Author contributions S.N. wrote the manuscript. D.S. reviewed the introduction, discussion, and conclusion sections. R.M. and H.H. reviewed the methodology and results sections. A.T. reviewed the abstract and ensured alignment of the entire manuscript. Before submission, all authors reviewed the document.

Funding This work was funded by Sida under Grant Agreement No 13394.

Availability of data and materials Data are provided in the supplementary information.

Declarations

Ethics approval and consent to participate All authors have read, understood, and have complied as applicable with the statement on "Ethical responsibilities of Authors' as found in the Instructions for Authors.

Competing interests The authors declare no competing interests.

Appendices

Appendix 1

See Table 3.

Table 3 Importance Value Index (IVI) of different tree species in the miombo woodlands of the Tabora and Sikonge districts in the Tabora Region, and the Mlele and Tanganyika districts in the Katavi Region

Species	Frequency	Density	Dominance	Frequency per cent	Density per cent	Dominance per cent	Importance value
Julbernardia globiflora	0.802632	918	34.77078	6.003937	11.00587	20.3509	37.36071
Brachystegia spiciformis	0.565789	669	19.29935	4.232283	8.020621	11.29567	23.54857
Diplorhynchus condylocarpon	0.756579	944	7.147837	5.659449	11.31759	4.18354	21.16058
Brachystegia longifolia	0.421053	515	13.51292	3.149606	6.17432	7.908943	17.23287
Brachystegia boehmii	0.506579	410	11.95554	3.78937	4.915478	6.99743	15.70228
Pseudolachnostylis maprouneifolia	0.657895	427	7.178169	4.92126	5.11929	4.201293	14.24184
Burkea africana	0.513158	283	7.298404	3.838583	3.392879	4.271665	11.50313
Terminalia sericea	0.526316	383	4.83207	3.937008	4.591776	2.82815	11.35693
Combretum zeyheri	0.467105	420	4.441658	3.494094	5.035367	2.599647	11.12911
Pericopsis angolensis	0.421053	172	7.120446	3.149606	2.062103	4.167508	9.379217
Combretum collinum	0.473684	210	3.701186	3.543307	2.517684	2.166258	8.227249
Pterocarpus angolensis	0.434211	206	3.668064	3.248031	2.469728	2.146872	7.864631
Uapaca kirkiana	0.046053	325	3.435412	0.344488	3.896415	2.010704	6.251607
Isoberlinia angolensis	0.164474	104	4.970631	1.230315	1.246853	2.909248	5.386416
Erythrophleum africanum	0.282895	90	2.676037	2.116142	1.079007	1.566251	4.7614
Lannea schimperi	0.328947	86	2.083796	2.46063	1.031051	1.21962	4.711301
Pterocarpus tinctorius	0.223684	110	2.897705	1.673228	1.318787	1.69599	4.688005
Hymenocardia acida	0.25	132	0.69855	1.870079	1.582544	0.408852	3.861475
Combretum molle	0.25	78	1.345967	1.870079	0.93514	0.787778	3.592996
Schrebera trichoclada	0.289474	84	0.613472	2.165354	1.007073	0.359058	3.531485
Crossopteryx febrifuga	0.164474	85	0.901871	1.230315	1.019062	0.527854	2.777231
Parinari curatellifolia	0.105263	43	1.641313	0.787402	0.515526	0.96064	2.263567
Cassipourea mollis	0.197368	43	0.334687	1.476378	0.515526	0.195888	2.187792
Ochna longipes	0.164474	48	0.39175	1.230315	0.575471	0.229286	2.035072
Strychnos pungens	0.125	43	0.768108	0.935039	0.515526	0.449564	1.900129
Oldfieldia dactylophylla	0.125	47	0.532399	0.935039	0.563482	0.311607	1.810128
Vitex mombassae	0.125	50	0.381974	0.935039	0.599449	0.223565	1.758053
Swartzia madagascariensis	0.111842	51	0.425633	0.836614	0.611437	0.249118	1.697169
Combretum psidioides	0.111842	37	0.566014	0.836614	0.443592	0.331281	1.611487
Albizia antunesiana	0.105263	23	0.92758	0.787402	0.275746	0.542901	1.606049
Hexalobus monopetalus	0.131579	35	0.246343	0.984252	0.419614	0.144182	1.548048
Maprounea africana	0.098684	49	0.371819	0.738189	0.58746	0.217621	1.54327
Monotes adenophyllus	0.059211	38	1.04757	0.442913	0.455581	0.613129	1.511624
Julbernardia paniculata	0.046053	52	0.923796	0.344488	0.623426	0.540686	1.508601
Isoberlinia tomentosa	0.039474	32	1.310307	0.295276	0.383647	0.766906	1.445829
Philenoptera violacea	0.085526	39	0.49333	0.639764	0.46757	0.28874	1.396073

Table 3 (continued)

Species	Frequency	Density	Dominance	Frequency per cent	Density per cent	Dominance per cent	Importance value
Xylopia antunesii	0.111842	31	0.300951	0.836614	0.371658	0.176143	1.384415
Terminalia mollis	0.098684	27	0.371307	0.738189	0.323702	0.217321	1.279213
Anisophyllea boehmii	0.078947	23	0.685069	0.590551	0.275746	0.400962	1.26726
Commiphora mossambicensis	0.098684	32	0.162811	0.738189	0.383647	0.095291	1.217127
Monotes elegans	0.052632	42	0.53572	0.393701	0.503537	0.31355	1.210788
Sclerocarya birrea	0.039474	7	1.336551	0.295276	0.083923	0.782266	1.161465
Diospyros kirkii	0.078947	27	0.415857	0.590551	0.323702	0.243396	1.157649
Margaritaria discoidea	0.085526	36	0.139067	0.639764	0.431603	0.081394	1.152761
Magnistipula butayei	0.046053	21	0.928122	0.344488	0.251768	0.543218	1.139475
Philenoptera eriocalyx	0.078947	23	0.440191	0.590551	0.275746	0.257638	1.123936
Dalbergia nitidula	0.092105	24	0.1876	0.688976	0.287735	0.1098	1.086512
Monotes africanus	0.059211	18	0.657981	0.442913	0.215801	0.385108	1.043823
Strychnos cocculoides	0.078947	28	0.160496	0.590551	0.335691	0.093936	1.020179
Catunaregam spinosa	0.078947	25	0.208613	0.590551	0.299724	0.122098	1.012374
Annona senegalensis	0.052632	35	0.189063	0.393701	0.419614	0.110656	0.923971
Ximenia caffra	0.078947	19	0.12635	0.590551	0.22779	0.073951	0.892293
Ozoroa insignis	0.065789	23	0.197176	0.492126	0.275746	0.115405	0.883277
Brachystegia bussei	0.039474	14	0.712516	0.295276	0.167846	0.417026	0.880148
Ximenia americana	0.065789	26	0.129722	0.492126	0.311713	0.075925	0.879764
Julbernardia unijugata	0.026316	11	0.853002	0.19685	0.131879	0.499251	0.827981
Dichrostachys cinerea	0.065789	23	0.083434	0.492126	0.275746	0.048833	0.816705
Combretum fragrans	0.046053	26	0.205269	0.344488	0.311713	0.120142	0.776343
Markhamia obtusifolia	0.059211	17	0.123238	0.442913	0.203812	0.07213	0.718856
Thespesia garckeana	0.032895	28	0.200861	0.246063	0.335691	0.117561	0.699316
Bauhinia petersiana	0.046053	18	0.124417	0.344488	0.215801	0.07282	0.63311
Holarrhena febrifuga	0.046053	18	0.076761	0.344488	0.215801	0.044927	0.605217
Phyllocosmus lemaireanus	0.026316	20	0.239253	0.19685	0.239779	0.140032	0.576661
Uapaca nitida	0.039474	13	0.174394	0.295276	0.155857	0.10207	0.553203
Psorospermum febrifugum	0.052632	11	0.031709	0.393701	0.131879	0.018559	0.544138
Xeroderris stuhlmannii	0.026316	6	0.46748	0.19685	0.071934	0.27361	0.542394
Flacourtia indica	0.046053	13	0.05915	0.344488	0.155857	0.03462	0.534965
Commiphora africana	0.052632	9	0.05051	0.393701	0.107901	0.029563	0.531164
Dalbergia boehmii	0.039474	10	0.178173	0.295276	0.11989	0.104282	0.519448
Diospyros fischeri	0.039474	11	0.152225	0.295276	0.131879	0.089095	0.51625
Strychnos potatorum	0.039474	11	0.121661	0.295276	0.131879	0.071207	0.498361
Ziziphus mucronata	0.032895	14	0.139441	0.246063	0.167846	0.081613	0.495522

Table 3 (continued)

Species	Frequency	Density	Dominance	Frequency per cent	Density per cent	Dominance per cent	Importance value
Multidentia crassa	0.046053	9	0.03294	0.344488	0.107901	0.01928	0.471669
Vitex doniana	0.026316	7	0.300402	0.19685	0.083923	0.175822	0.456595
Brachystegia floribunda	0.019737	9	0.306532	0.147638	0.107901	0.17941	0.434948
Brachystegia manga	0.006579	7	0.443211	0.049213	0.083923	0.259406	0.392541
Boscia salicifolia	0.019737	4	0.33608	0.147638	0.047956	0.196703	0.392297
Bridelia cathartica	0.032895	8	0.059067	0.246063	0.095912	0.034571	0.376546
Zanthoxylum deremense	0.006579	5	0.453026	0.049213	0.059945	0.265151	0.374308
Afzelia quanzensis	0.026316	4	0.203001	0.19685	0.047956	0.118814	0.36362
Combretum apiculatum	0.032895	7	0.040846	0.246063	0.083923	0.023907	0.353893
Phyllanthus engleri	0.026316	8	0.102133	0.19685	0.095912	0.059777	0.352539
Cassia abbreviata	0.026316	6	0.142231	0.19685	0.071934	0.083246	0.35203
Zahna africana	0.026316	7	0.117176	0.19685	0.083923	0.068582	0.349355
Euphorbia matabelensis	0.013158	18	0.059533	0.098425	0.215801	0.034844	0.349071
Faurea rochetiana	0.013158	10	0.22046	0.098425	0.11989	0.129033	0.347348
Rothmannia engleriana	0.026316	10	0.040961	0.19685	0.11989	0.023974	0.340714
Brachystegia glaberrima	0.019737	13	0.063134	0.147638	0.155857	0.036952	0.340446
Albizia adianthifolia	0.026316	6	0.096272	0.19685	0.071934	0.056347	0.325131
Chrysophyllum bangweolense	0.026316	6	0.09019	0.19685	0.071934	0.052787	0.321571
Grewia bicolor	0.019737	12	0.037	0.147638	0.143868	0.021656	0.313161
Strychnos innocua	0.026316	6	0.039403	0.19685	0.071934	0.023062	0.291847
Dombeya rotundifolia	0.026316	5	0.031256	0.19685	0.059945	0.018294	0.275089
Vangueriopsis lanciflora	0.026316	5	0.023727	0.19685	0.059945	0.013887	0.270682
Securidaca longipedunculata	0.026316	4	0.040774	0.19685	0.047956	0.023864	0.268671
Commiphora mollis	0.013158	6	0.157032	0.098425	0.071934	0.091909	0.262268
Uapaca sansibarica	0.019737	5	0.065142	0.147638	0.059945	0.038127	0.24571
Rhus vulgaris	0.019737	6	0.040655	0.147638	0.071934	0.023795	0.243366
Kigelia africana	0.013158	5	0.143178	0.098425	0.059945	0.0838	0.24217
Strychnos spinosa	0.019737	5	0.040008	0.147638	0.059945	0.023416	0.230999
Allophylus africanus	0.013158	8	0.057287	0.098425	0.095912	0.033529	0.227866
Piliostigma thonningii	0.019737	5	0.030848	0.147638	0.059945	0.018055	0.225638
Syzygium owariensis	0.019737	5	0.014149	0.147638	0.059945	0.008281	0.215864
Faurea saligna	0.013158	4	0.106642	0.098425	0.047956	0.062416	0.208797
Erythrina abyssinica	0.019737	3	0.035601	0.147638	0.035967	0.020837	0.204442
Maytenus senegalensis	0.019737	4	0.014469	0.147638	0.047956	0.008468	0.204062
Pavetta schumanniana	0.019737	4	0.010637	0.147638	0.047956	0.006226	0.20182
Clerodendrum myricoides	0.013158	7	0.019712	0.098425	0.083923	0.011537	0.193885

Table 3 (continued)

Species	Frequency	Density	Dominance	Frequency per cent	Density per cent	Dominance per cent	Importance value
Canthium burtii	0.013158	7	0.016628	0.098425	0.083923	0.009732	0.19208
Albizia amara	0.013158	3	0.090156	0.098425	0.035967	0.052767	0.187159
Dracaena mannii	0.013158	4	0.028019	0.098425	0.047956	0.016399	0.16278
Diospyros mespiliformis	0.013158	2	0.058591	0.098425	0.023978	0.034292	0.156696
Maerua angolensis	0.013158	3	0.022462	0.098425	0.035967	0.013147	0.147539
Ekebergia benguelensis	0.013158	3	0.020175	0.098425	0.035967	0.011808	0.1462
Cussonia arborea	0.013158	2	0.034558	0.098425	0.023978	0.020227	0.14263
Diospyros zombensis	0.013158	3	0.010531	0.098425	0.035967	0.006163	0.140556
Senegalia goetzei	0.006579	5	0.04458	0.049213	0.059945	0.026092	0.13525
Sterculia quinqueloba	0.013158	2	0.019315	0.098425	0.023978	0.011305	0.133708
Vangueria infausta	0.013158	2	0.010681	0.098425	0.023978	0.006252	0.128655
Hymenodictyon floribundum	0.006579	5	0.01996	0.049213	0.059945	0.011682	0.12084
Vachellia nilotica	0.006579	1	0.090259	0.049213	0.011989	0.052827	0.114029
Tarenna pavettoides	0.006579	2	0.037036	0.049213	0.023978	0.021677	0.094867
Tricalysia acocantheroides	0.006579	2	0.025524	0.049213	0.023978	0.014939	0.088129
Vachellia sieberiana	0.006579	1	0.045239	0.049213	0.011989	0.026478	0.087679
Ziziphus abyssinica	0.006579	2	0.023192	0.049213	0.023978	0.013574	0.086765
Brachystegia utilis	0.006579	2	0.012093	0.049213	0.023978	0.007078	0.080268
Ficus ingens	0.006579	1	0.032047	0.049213	0.011989	0.018757	0.079959
Ormocarpum kirkii	0.006579	2	0.008408	0.049213	0.023978	0.004921	0.078111
Antidesma venosum	0.006579	2	0.006195	0.049213	0.023978	0.003626	0.076817
Vangueria volkensii	0.006579	2	0.005507	0.049213	0.023978	0.003223	0.076414
Memecylon flavovirens	0.006579	2	0.005395	0.049213	0.023978	0.003158	0.076348
Stereospermum kunthianum	0.006579	2	0.004886	0.049213	0.023978	0.00286	0.07605
Zanthoxylum chalybeum	0.006579	1	0.016061	0.049213	0.011989	0.0094	0.070602
Sterculia mhosya	0.006579	1	0.01307	0.049213	0.011989	0.00765	0.068851
Vachellia drepanolobium	0.006579	1	0.01131	0.049213	0.011989	0.006619	0.067821
Albizia tanganyicensis	0.006579	1	0.008171	0.049213	0.011989	0.004783	0.065984
Pleurostylia africana	0.006579	1	0.00694	0.049213	0.011989	0.004062	0.065263
Ehretia amoena	0.006579	1	0.006362	0.049213	0.011989	0.003723	0.064925
Sterculia africana	0.006579	1	0.005675	0.049213	0.011989	0.003321	0.064523
Albizia harveyi	0.006579	1	0.005027	0.049213	0.011989	0.002942	0.064144
Uvaria sp	0.006579	1	0.004072	0.049213	0.011989	0.002383	0.063585
Gardenia jovis-tonantis	0.006579	1	0.003117	0.049213	0.011989	0.001824	0.063026
Vitex ferruginea	0.006579	1	0.003019	0.049213	0.011989	0.001767	0.062969
Commiphora lindensis	0.006579	1	0.002376	0.049213	0.011989	0.001391	0.062592

Table 3 (continued)

Species	Frequency	Density	Dominance	Frequency per cent	Density per cent	Dominance per cent	Importance value
Friesodielsia obovata	0.006579	1	0.002124	0.049213	0.011989	0.001243	0.062445
Ochna schweinfurthiana	0.006579	1	0.002124	0.049213	0.011989	0.001243	0.062445
Commiphora ugogensis	0.006579	1	0.001963	0.049213	0.011989	0.001149	0.062351

Appendix 2

See Table 4.

Table 4 Error matrices

Classifications	Crown of the tree species						
		Julbernardia globiflora	*Brachystegia spiciformis*	*Pterocarpus tinctorius*	Others	Total	User Accuracy (%)
March	*Julbernardia globiflora*	23	9	3	3	38	60.52
	Brachystegia spiciformis	8	20	6	2	36	55.56
	Pterocarpus tinctorius	6	3	7		16	43.75
	Others	1	1	0	2	4	50.00
	Total	38	33	16	7	94	
	Producer Accuracy (%)	60.53	60.61	43.75	28.57		
July	*Julbernardia globiflora*	30	2	7	4	43	69.77
	Brachystegia spiciformis	3	30	7	1	41	73.17
	Pterocarpus tinctorius	6	1	1	1	9	11.11
	Others	0	1	0	1	2	50.00
	Total	39	34	15	7	95	
	Producer Accuracy (%)	76.92	88.24	6.67	14.29		
September	*Julbernardia globiflora*	34	5	4	5	48	70.83
	Brachystegia spiciformis	1	26	8		35	74.29
	Pterocarpus tinctorius	3	2	4	1	10	40.00
	Others	0	0	0	1	1	100.00
	Total	38	33	16	7	94	
	Producer Accuracy (%)	89.47	78.79	25	14.29		
March and July	*Julbernardia globiflora*	34	4	6	3	47	72.34
	Brachystegia spiciformis	3	29	6	2	40	72.50
	Pterocarpus tinctorius	2	0	4	1	7	57.14
	Others	0	0	0	1	1	100.00
	Total	39	33	16	7	95	
	Producer Accuracy (%)	87.18	87.88	25	14.29		
March and September	*Julbernardia globiflora*	37	6	5	5	53	69.81
	Brachystegia spiciformis	1	26	7	1	35	74.29
	Pterocarpus tinctorius	1	1	4	0	6	66.67
	Others	0	0	0	1	1	100.00
	Total	39	33	16	7	95	
	Producer Accuracy (%)	94.87	78.79	25	14.29		
July and September	*Julbernardia globiflora*	32	6	7	5	50	64.00
	Brachystegia spiciformis	1	28	6	1	36	77.78
	Pterocarpus tinctorius	6	0	3		9	33.33
	Others	0	0	0	1	1	100.00
	Total	39	34	16	7	96	
	Producer Accuracy (%)	82.05	82.35	18.75	14.29		
March, July and September	*Julbernardia globiflora*	34	5	7	5	51	66.67
	Brachystegia spiciformis	1	28	7	1	37	75.68
	Pterocarpus tinctorius	3	0	2	0	5	40.00
	Others	1	0	0	1	2	50.00
	Total	39	33	16	7	95	
	Producer Accuracy (%)	87.18	84.85	12.5	14.29		

References

1. Frost P. The ecology of Miombo woodlands," in The Miombo in Transition: Woodlands and Welfare in Africa, no. June, B. Campbell, Ed. Bogor, Indonesia: Center for International Forestry Research (CIFOR), 1996, pp. 11–57.
2. Dziba L, et al. Scenarios for just and sustainable futures in the Miombo woodlands, Miombo woo. Switzeland: Springer; 2020.
3. Abdallah J, Monela G. Overview of Miombo woodlands in Tanzania. In: Proc. First MITMIOMBO Proj. Work. shop, vol. 50, no. February, pp. 9–23, 2007, [Online]. Available: http://www.metla.eu/julkaisut/workingpapers/2007/mwp050-02.pdf.
4. Syampungani S, Chirwa PW, Akinnifesi FK, Sileshi G, Ajayi OC. The Miombo woodlands at the cross roads: potential threats, sustainable livelihoods, policy gaps and challenges. Nat Resour Forum. 2009;33(2):150–9. https://doi.org/10.1111/j.1477-8947.2009.01218.x.
5. Dewees P et al. Managing the Miombo Woodlands of Southern Africa: Policies, incentives, and options for the rural poor. Washington, DC: Program on Forests (PROFOR), 2011.
6. Lusambo LP. Economics on the Household energy in miombo woodlands of Eastern and Southern Tanzania. University of Bangor; 2009.
7. URT, National Forest Resources Monitoring and Assessment of Tanzania Mainland: Main Results. Dar Es Salaam: United Republic of Tanzania, Ministry of Natural Resources and Tourism. Dar Es Salaam, 2015.
8. Jew EKK, Dougill AJ, Sallu SM, Connell JO, Benton TG. Forest ecology and management miombo woodland under threat: consequences for tree diversity and carbon storage. For Ecol Manage. 2016;361:144–53. https://doi.org/10.1016/j.foreco.2015.11.011.
9. Chidumayo EN. Management implications of tree growth patterns in miombo woodlands of Zambia. For Ecol Manag. 2019;436:105–16. https://doi.org/10.1016/j.foreco.2019.01.018.
10. Grime J. Benefits of plant diversity to ecosystems: immediate, filter and founder effects. J Ecol. 1998;86:902–10.
11. John E, Bunting P, Hardy A, Roberts O, Giliba R, Silayo DS. Modelling the impact of climate change on Tanzanian forests. Divers Distrib. 2020;26(12):1663–86. https://doi.org/10.1111/ddi.13152.
12. Jinga P, Palagi J. Dry and wet miombo woodlands of south-central Africa respond differently to climate change. Environ Monit Assess. 2020;192(372):1–16. https://doi.org/10.1007/s10661-020-08342-x.
13. O'Connor B, et al. Earth observation as a tool for tracking progress towards the Aichi biodiversity targets. Remote Sens Ecol Conserv. 2015;1(1):19–28. https://doi.org/10.1002/rse2.4.
14. Pu R. Mapping tree species using advanced remote sensing technologies: a state-of-the-art review and perspective. J Remote Sens. 2021. https://doi.org/10.34133/2021/9812624.
15. Shamaoma H, et al. Use of multi-date and multi-spectral UAS imagery to classify dominant tree species in the wet Miombo woodlands of Zambia. Sensors. 2023. https://doi.org/10.3390/s23042241.
16. Dixon DJ, Callow JN, Duncan JMA, Setterfield SA, Pauli N. Satellite prediction of forest flowering phenology. Remote Sens Environ. 2021. https://doi.org/10.1016/j.rse.2020.112197.
17. Cho MA, et al. Mapping tree species composition in South African savannas using an integrated airborne spectral and LiDAR system. Remote Sens Environ. 2012;125:214–26. https://doi.org/10.1016/j.rse.2012.07.010.
18. Adelabu S, Dube T. Employing ground and satellite-based QuickBird data and random forest to discriminate five tree species in a Southern African Woodland. Geocarto Int. 2015;30(4):457–71. https://doi.org/10.1080/10106049.2014.885589.
19. Madonsela S, et al. Multi-phenology WorldView-2 imagery improves remote sensing of savannah tree species. Int J Appl Earth Obs Geoinf. 2017;58:65–73. https://doi.org/10.1016/j.jag.2017.01.018.
20. van Deventer H, Cho MA, Mutanga O. Multi-season RapidEye imagery improves the classification of wetland and dryland communities in a subtropical coastal region. ISPRS J Photogramm Remote Sens. 2019;157(February):171–87. https://doi.org/10.1016/j.isprsjprs.2019.09.007.
21. Lake TA, Briscoe Runquist RD, Moeller DA. Deep learning detects invasive plant species across complex landscapes using Worldview-2 and Planetscope satellite imagery. Remote Sens Ecol Conserv. 2022;8(6):875–89. https://doi.org/10.1002/rse2.288.
22. Fick SE, Hijmans RJ. WorldClim 2: new 1-km spatial resolution climate surfaces for global land areas. Int J Climatol. 2017;37(12):4302–15. https://doi.org/10.1002/joc.5086.
23. Han H, Guo X, Yu H. Variable selection using mean decrease accuracy and mean decrease gini based on random forest. In: 2016 7th IEEE Int. Conf. Softw. Eng. Serv. Sci., pp. 219–224, 2016, https://doi.org/10.1109/ICSESS.2016.7883053.
24. Behnamian A, Millard K, Banks SN, White L, Richardson M, Pasher J. A systematic approach for variable selection with random forests : achieving stable variable importance values. IEEE Geosci Remote Sens Lett. 2017;14(11):1988–92. https://doi.org/10.1109/lgrs.2017.2745049.
25. Cutler R, et al. Random forests for classification in ecology. Ecology. 2007;88(11):2783–92.
26. Zur Y, Gitelson OB, Chivkunova, Merzlyak MN. The spectral contribution of carotenoids to light absorption and reflectance in green leaves. In: Proc. 2nd Int. Conf. Geospatial Inf. Agric. For. Buena Vista, FL, January 10–12, vol. 2, pp. 1–7, 2000, [Online]. Available: http://digitalcommons.unl.edu/natrespapers/272/
27. Cho MA, Debba P, Mathieu R, Naidoo L, Van Aardt J, Asner GP. Improving discrimination of savanna tree species through a multiple-endmember spectral angle mapper approach: Canopy-level analysis. IEEE Trans Geosci Remote Sens. 2010;48(11):4133–42. https://doi.org/10.1109/TGRS.2010.2058579.
28. Karlson M, Ostwald M, Reese H, Bazié HR, Tankoano B. Assessing the potential of multi-seasonal WorldView-2 imagery for mapping West African agroforestry tree species. Int J Appl Earth Obs Geoinf. 2016;50:80–8. https://doi.org/10.1016/j.jag.2016.03.004.
29. Nasiri V, Beloiu M, Asghar Darvishsefat A, Griess VC, Maftei C, Waser□, LT. Mapping tree species composition in a Caspian temperate mixed forest based on spectral-temporal metrics and machine learning. Int J Appl Earth Obs Geoinf. 2023;116:103154. https://doi.org/10.1016/j.jag.2022.103154.